Low-Complexity Channel Estimation and Passive Beamforming for RIS-Assisted MIMO Systems Relying on Discrete Phase Shifts

Jiancheng An, Chao Xu, *Senior Member, IEEE,* Lu Gan, and Lajos Hanzo, *Fellow, IEEE*

Abstract—**Reconfigurable intelligent surfaces (RISs) are capable of enhancing the capacity of wireless networks at a low cost. In practical RIS-assisted communication systems, the acquisition of channel state information (CSI) and RIS reflection optimization constitute a pair of challenges. In this paper, a low-complexity channel estimation and passive beamforming design is proposed.** *First of all*, **we conceive a low-complexity framework for maximizing the achievable rate of RIS-assisted multiple-input multiple-output (MIMO) systems having discrete phase shifts at each RIS element. In contrast to existing solutions, the proposed arrangement partitions the channel training stage into several phases, where the RIS reflection coefficients are pre-designed and the effective superposed channel is estimated instead of separately training the source-destination and source-RIS-destination links. Based on this, the active beamformer can be designed at low complexity and the RIS reflection optimization is performed by selecting that one from the pre-designed training set which maximizes the achievable rate.** *Secondly*, **we propose novel techniques for generating the training set of RIS reflection coefficients. The theoretical performance of the proposed scheme is analyzed and compared to the optimal RIS configuration.** *Finally*, **our simulation results demonstrate that the proposed framework is more competitive than its existing counterparts when relying on imperfect CSI, especially for rapidly time-varying channels having short channel coherence time.**

Index Terms—**Reconfigurable intelligent surface (RIS), channel estimation, passive beamforming, transmit precoding, intelligent reflecting surface (IRS), multiple-input multiple-output (MIMO).**

I. INTRODUCTION

RECENTLY, reconfigurable intelligent surfaces (RIS) [1]–[4], which are also known as intelligent reflecting surfaces (IRS) [5] and large intelligent surfaces (LIS) [6], have attracted substantial research attention [7], [8]. Specifically, a RIS is a planar meta-surface constructed of a large number of reflecting elements, each of which can be reconfigured to impose individual phase shifts onto the incident signals [9]. As a result, the radio propagation environments can be customized according to the specific quality of service

(QoS) requirements [4], [10]. In contrast to classic cooperative communications relying on active relays, the RIS elements passively perform signal reflection without employing any active radio frequency (RF) chains, hence reducing the power consumption and transmission delay [11], [12]. Some recent studies have demonstrated that a RIS using large metasurfaces is capable of outperforming decode/amplify-and-forward relaying despite their lower complexity [13]. Furthermore, RISs are also capable of operating in a full-duplex (FD) mode without encountering the self-interference problem in active relays [5], [12]. Moreover, light-weight and low-cost RISs are easy to install on and remove from the environment objects [10]. Due to the aforementioned benefits, RISs are considered to be an attractive candidate for power-efficient next-generation green wireless communications [8], [14].

Nevertheless, some new technical challenges have emerged in RIS-empowered wireless communication systems. On one hand, one of the major challenges is the acquisition of the channel state information (CSI) due to the absence of baseband signal processing capability at the RIS [4], [5], [10], [15]. Hence, the channels of the access point (AP)-RIS link and the RIS-user equipment (UE) link can no longer be estimated separately by conventional pilot-based approaches. To solve this problem, several novel methods have been proposed for estimating the cascaded AP-RIS-UE channels instead [16]–[18]. For example, in [16], the simple ON/OFF method was proposed, where the direct and reflected channels are estimated by switching on/off the RIS elements in sequence. Furthermore, a discrete Fourier transformation (DFT) matrix-based solution was employed in [17] for optimizing the RIS reflection coefficients during the channel estimation phase, which is capable of minimizing the mean square error (MSE) of the channel estimates. More recently, an optimal pilot power allocation strategy was proposed in [18] for improving the throughput attained by RIS-assisted communication systems having imperfect CSI. However, the aforementioned methods require the same number of pilot symbols as that of the reflecting elements at the RIS, which becomes excessive for a massive number of reflecting elements. To overcome this limitation, a novel three-phase channel estimation method was proposed in [19] for reducing the number of pilot symbols by exploiting the commonality of the AP-RIS link between multiple UEs. As a further advance, the authors of [20] exploited the beamspace sparsity of the AP-RIS link for further reducing the pilot overhead. Later, You *et al.* [21] reduced the number of pilots by grouping several RIS elements into a bundle having

TABLE I
THE CONTRIBUTION OF THE PROPOSED LOW-COMPLEXITY FRAMEWORK COMPARED TO EXISTING SOLUTIONS FOR RIS-ASSISTED SYSTEMS.

Contributions	*	[11]-2019	[12]-2019	[24]-2020	[44]-2020	[23]-2020	[32]-2021
Reduced set of reflection phase shifts	✓	×	×	×	×	×	×
Superposed channel's estimation	✓	×	×	×	×	×	×
Low-complexity passive beamforming design	✓	×	×	✓	✓	✓	✓
Flexibility in the number of pilots	✓	×	×	×	×	×	✓
Reduction in the backhaul overhead	✓	×	×	×	×	×	×
Theoretical analysis	✓	×	✓	×	×	✓	×
MIMO setup	MIMO	MU-MISO	MU-MISO	MIMO	MC/Network-MIMO	MU-MISO	MIMO
Phase-shift model	Discrete	Continuous	Continuous	Continuous	Continuous	Discrete	Continuous
Optimization objective	Throughput	EE/Sum rate	Transmit power	Throughput	WSR	Transmit power	EE/Rate

MU: multiple user;   EE: energy efficiency;   MC: multiple cell;   WSR: weighted sum rate;

a joint channel, albeit at the cost of a performance penalty. As a benefit, the number of pilots is reduced. The motivated reader may refer to [10], [15], [22] and the references therein for comprehensive surveys on the existing channel estimation techniques designed for RIS-assisted communication systems.

On the other hand, the beneficial configuration of both the transmit beamforming weights and the RIS reflection coefficients constitutes another major challenge in practical RIS-assisted wireless systems [12], [23]–[33]. In [12] and [23], Wu *et al.* studied joint passive beamforming at the RIS and transmit beamforming at the AP in multiuser multiple-input multiple-output (MIMO) scenarios, where the popular alternating optimization (AO) method based on semidefinite relaxation (SDR) was applied for finding high-quality approximate RIS reflection coefficients and transmit beamforming vectors for multiple users. Moreover, the RIS configuration of point-to-point MIMO systems has been optimized in [24] in terms of maximizing the MIMO channel capacity. Specifically, the optimization of the RIS reflection coefficients and the transmit covariance matrix were performed alternately, where the optimal closed-form solution of each objective is derived assuming that the other was already determined. Following this, the authors of [25] investigated the weighted sum-rate maximizing problem in a multiuser scenario, where practical RIS elements having discrete phase shifts were considered. More recently, the authors of [27] presented a beneficial phase shift design by maximizing a tight upper bound of the spectral efficiency, where only statistical CSI is available. Furthermore, the channel correlation has also been developed to further simplify the reflection optimization [28], [29]. In addition, the optimization of the RIS reflection coefficients has been carried out in combination with other emerging communication technologies, such as physical layer security [34], [35], millimeter-wave communications [36], unmanned aerial vehicles (UAV) [37], [38], index modulation (IM) [39], deep learning [40], non-orthogonal multiple access (NOMA) [41], simultaneous wireless information and power transfer (SWIPT) [42], [43] and cell-free massive MIMO [45].

In a nutshell, substantial research efforts have been invested in the channel estimation and reflection coefficient optimization of RIS-assisted systems. Nonetheless, the existing methods still exhibit limitations. For instance, the number of pilot symbols required for estimating the cascaded AP-RIS-UE channels is proportional to the number of RIS elements [17], [19]. Furthermore, the RIS configuration requires the joint design of the transmit beamforming at the AP and the reflection coefficients optimization at the RIS [12], [23]. These issues have to be addressed for the practical implementation of the RIS. *Against this background, in this paper, we propose a novel low-complexity channel estimation and passive beamforming design, which provides flexible trade-offs concerning the pilot overhead, backhaul requirement, system performance, and implementation complexity.* More specifically, the novel contributions of this paper are boldly and explicitly contrasted to the literature in Table I and are summarized as follows:

- First of all, we conceive a low-complexity channel estimation and passive beamforming framework for maximizing the achievable rate of RIS-assisted MIMO systems having discrete phase shifts at each RIS element. Specifically, the proposed arrangement partitions the channel training phase into several periods, where the reflection coefficients at the RIS are pre-configured according to our specific configuration method. The effective superposed channel combining the direct link and all reflected links are then directly estimated instead of using separate training for each link. Based on this, on one hand, the active beamforming weights at the transmitter can be designed at low complexity. On the other hand, the optimization of the RIS reflection coefficients is simplified by selecting that particular one from the pre-designed training set which maximizes the achievable rate.
- Secondly, we propose novel configuration approaches for generating a suitable training set of the RIS reflection coefficients during the channel training phase, namely, a random configuration and a Euclidean distance maximization based configuration, explicitly the first approach randomly generates RIS reflection coefficients from the feasible set determined by discrete phase shifts, while the second one endeavors to maximize the Euclidean distance of all pairs of legitimate RIS reflection coefficient vectors in the training set. Furthermore, the theoretical performance of the proposed scheme is analyzed in terms of the average received power for a single-input single-output (SISO) scenario and it is compared to the optimal RIS configuration. Our theoretical analysis demonstrates that the proposed framework only imposes a moderate performance erosion compared to the optimal RIS configuration, despite its substantially reduced complexity compared to the conventional solutions.
- Thirdly, the advantages of the proposed low-complexity

channel estimation and passive beamforming framework are demonstrated over the conventional solutions in terms of reducing both the complexity as well as the pilot overhead and the signaling requirements. In addition, the proposed scheme is independent of the specific reflected channel models, which can be flexibly applied to various scenarios.

The rest of this paper is structured as follows. Section II and Section III introduce the system model of RIS-assisted MIMO systems as well as existing channel estimation and passive beamforming paradigms, respectively. Following this, the proposed low-complexity framework is presented in Section IV. In Section V, the method of generating the training set of RIS reflection coefficients and our theoretical analysis are detailed, while the potential benefits of the proposed framework are discussed in Section VI. Section VII provides our numerical results for evaluating the proposed scheme. Finally, Section VIII concludes the paper.

Notations: We use upper/lower bold face letters to indicate matrices/vectors; scalars are denoted by italic letters; $(\cdot)^T$ and $(\cdot)^H$ represent transpose and Hermitian transpose, respectively; $\mathbf{S}^{-1}$, $\mathrm{tr}(\mathbf{S})$ and $\det(\mathbf{S})$ denote the inverse, trace and determinant of the square matrix $\mathbf{S}$, respectively; $\mathrm{diag}(\mathbf{v})$ denotes the diagonal matrix with each diagonal element being the corresponding element in $\mathbf{v}$; we denote the $N \times N$ identity matrix as $\mathbf{I}_N$; $\mathbf{1}$ denotes an all-one vector with appropriate dimensions; $\|\cdot\|$ is the Frobenius norm of a complex vector; furthermore, $\mathbb{E}\{\cdot\}$ stands for the expected value; $\lceil \cdot \rceil$ and $\otimes$ represent the ceiling operation and Kronecker product, respectively, $\log(\cdot)$ represents the logarithmic function; $|z|$ and $\angle z$ denote the magnitude and phase of a complex number z, respectively; $a!$ denotes the factorial of the non-negative integer a. $\mathbf{M}_{a:b,c:d}$ represents the elements of the $a \sim b$th rows and $c \sim d$th columns extracted from the matrix $\mathbf{M}$, the distribution of a circularly symmetric complex Gaussian (CSCG) random vector with mean vector $\mathbf{v}$ and covariance matrix $\mathbf{\Sigma}$ is denoted by $\sim \mathcal{CN}(\mathbf{v}, \mathbf{\Sigma})$, where $\sim$ stands for "distributed as"; $\sim \mathcal{U}(\mathcal{S})$ denotes the uniformly distribution in a set $\mathcal{S}$; $\mathbb{C}^{x \times y}$ denotes the space of $x \times y$ complex-valued matrices; C_n^k denotes the number of arrangements choosing k from n.

II. SYSTEM MODEL

Let us consider the point-to-point MIMO system of Fig. 1, where a RIS equipped with M reflecting elements is employed for enhancing the communications link spanning from an AP having N_a antennas to a UE with N_u antennas. Each RIS element reflects the signal with an individual phase shift, i.e., θ_m, $m = 1, \cdots, M$, which can be dynamically adjusted by the RIS controller for beneficially controlled signal reflection[1]. For the sake of practical implementation, the phase shift of each RIS element are assumed to be one of $B = 2^b$ discrete values, where b denotes the number of bits used for quantizing the phase shift levels. For simplicity, we assume that the discrete phase shifts are obtained by uniformly quantizing the

---

[1]Note that in this paper, we only consider the phase shift design at each RIS element. The magnitude of each RIS reflection coefficient is set to be 1 in order to maintain maximum signal power reflection [12].
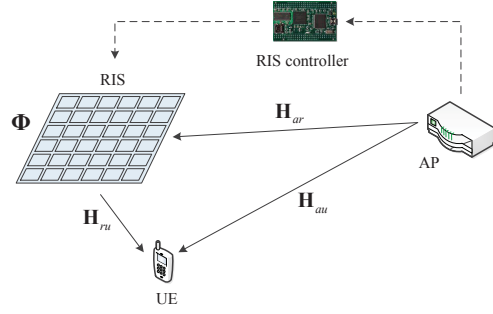

Fig. 1. Schematic of a RIS-assisted MIMO communication system.

interval $[0, 2\pi)$. Thus, the set of discrete phase shifts at each RIS element is given by

$$\mathcal{B} = \{0, \Delta\theta, \cdots, (B-1)\Delta\theta\}, \tag{1}$$

where $\Delta\theta = 2\pi/B$. Let $\varphi_m = e^{j\theta_m}$ denote the reflection coefficient at the mth RIS element, the phase of each φ_m is constrained by $\theta_m \in \mathcal{B}$, $m = 1, \cdots, M$.

In this paper, we consider non-dispersive communications over quasi-static block-fading channels and adopt the time-division duplex (TDD) mode. Let $\mathbf{H}_{au} \in \mathbb{C}^{N_u \times N_a}$ represent the complex baseband channel matrix of the direct link spanning from the AP to the UE, $\mathbf{H}_{ar} \in \mathbb{C}^{M \times N_a}$ as that of the AP-RIS link, and $\mathbf{H}_{ru} \in \mathbb{C}^{N_u \times M}$ as that of the RIS-UE link. Let $\mathbf{\Phi} = \mathrm{diag}(\boldsymbol{\varphi}) \in \mathbb{C}^{M \times M}$ denote the diagonal reflection coefficient matrix at the RIS, with $\boldsymbol{\varphi} = [\varphi_1, \cdots, \varphi_M]$. Therefore, the effective superimposed channel spanning from the AP to the UE is given by $\mathbf{H} = \mathbf{H}_{au} + \mathbf{H}_{ru}\mathbf{\Phi}\mathbf{H}_{ar}$.

We first consider channel estimation in the uplink phase. Let $\mathbf{x} \in \mathbb{C}^{N_u \times 1}$ denote the normalized pilot vector transmitted from the UE to the AP, i.e., $\mathbb{E}\{\|\mathbf{x}\|^2\} = 1$. The baseband signal $\mathbf{y} \in \mathbb{C}^{N_a \times 1}$ received at the AP is the superposition of that via the direct link and of the reflected links, which can be expressed as

$$\mathbf{y} = \mathbf{H}^H \sqrt{P_{UL}}\mathbf{x} + \mathbf{z} = \left(\mathbf{H}_{au}^H + \mathbf{H}_{ar}^H \mathbf{\Phi}^H \mathbf{H}_{ru}^H\right)\sqrt{P_{UL}}\mathbf{x} + \mathbf{z}, \tag{2}$$

where P_{UL} is the average power of the pilot symbols, $\mathbf{z}$ denotes the additive white Gaussian noise (AWGN) at the AP, which is of CSCG distribution, i.e., $\mathbf{z} \sim \mathcal{CN}(\mathbf{0}, \sigma_z^2 \mathbf{I}_{N_a})$.

In the downlink phase of data transmission, we denote the signal vector transmitted from the AP to the UE as $\mathbf{s} \in \mathbb{C}^{N_a \times 1}$. The transmit signal covariance matrix is thus defined by $\mathbf{S} = \mathbb{E}\{\mathbf{s}\mathbf{s}^H\} \in \mathbb{C}^{N_a \times N_a}$, with $\mathbf{S} \succeq \mathbf{0}$. We consider the average sum power constraint at the AP given by $\mathbb{E}\{\|\mathbf{s}\|^2\} = \mathrm{tr}(\mathbf{S}) \leq P_{DL}$. Hence, the signal vector $\mathbf{r} \in \mathbb{C}^{N_u \times 1}$ received by the UE is given by

$$\mathbf{r} = \mathbf{H}\mathbf{s} + \mathbf{n} = (\mathbf{H}_{au} + \mathbf{H}_{ru}\mathbf{\Phi}\mathbf{H}_{ar})\mathbf{s} + \mathbf{n}, \tag{3}$$

where $\mathbf{n} \sim \mathcal{CN}(\mathbf{0}, \sigma_n^2 \mathbf{I}_{N_u})$ denotes the independent CSCG vector at the UE, with σ_n^2 denoting the average noise power.

III. EXISTING CHANNEL ESTIMATION AND PASSIVE BEAMFORMING DESIGN

In this section, we will survey the existing channel estimation and passive beamforming designs conceived for RIS-assisted MIMO systems. Specifically, three channel estimation methods designed for the direct and reflected links are

introduced in Section III-A, some of which are appropriately adapted from that of SISO or multi-user multiple-input single-output (MISO) scenarios. Furthermore, the optimization of the RIS reflection coefficients in terms of maximizing the achievable rate based on the estimated CSI is presented in Section III-B.

A. Channel Estimation for RIS-assisted MIMO Communication Systems

1) The ON/OFF method: The most common channel estimation method for RIS-assisted communication systems is the ON/OFF method, which estimates the direct channel and reflected channels one after the other [16]. More specifically, the direct channel between the AP and the UE is first estimated upon muting all RIS elements. Based on the estimated direct channel coefficients, the cascaded AP-RIS-UE channels can be estimated by only switching on a single RIS element in each time slot (TS). After switching on all the reflecting elements in turn, the $(M+1)$ channel vectors corresponding to each of the transmit antenna (TA) are estimated. Following this, upon designing orthogonal pilot vectors for each of the different TAs, all the channel coefficients will be estimated within a total of $(M+1)N_u$ TSs.

2) The three-phase method: It is worth noting that the power loss of the ON/OFF method is severe due to the frequent switching of the RIS elements. To solve this problem, Wang *et al.* [19] proposed a three-phase channel estimation framework for RIS-assisted multiuser scenarios, which can be readily adjusted for point-to-point MIMO systems. Specifically, in the first phase, all the reflecting elements of the RIS are switched off for estimating the direct channel, which follows a similar philosophy as the ON/OFF method. In the second phase, all the RIS elements are switched on, and merely one typical TA of the UE, say TA 1, transmits pilot symbols for estimating the reflected channels by Antenna 1 to the AP. Finally, since the reflected channels corresponding to N_u antennas share the same AP-RIS link, the scaling characteristics of the reflected channels between multiple TAs makes it possible to estimate the remaining reflected channels within $\max\left(N_u-1, \lceil(N_u-1)M/N_a\rceil\right)$ TSs. The detailed procedures are given in [19], which are omitted here for the sake of brevity, but the authors verified that $N_u+M+\max\left(N_u-1, \lceil(N_u-1)M/N_a\rceil\right)$ pilot symbols provide sufficient degrees of freedom for estimating all the channel coefficients involved in Fig. 1.

3) The DFT-based method: However, the reduction of the number of pilots in the three-phase method is achieved at the cost of error propagation. More explicitly, the *quality* of the channel estimates in the subsequent phase depends heavily on the channel estimation accuracy of the previous phases. To overcome this disadvantage, we conceive a generalized DFT-based channel estimation method for RIS-assisted MIMO systems by extending the method of [17], which was designed for MISO scenarios. It has been shown in [17] that the DFT-based optimization of the RIS reflection coefficients achieves the Cramer-Rao lower bound (CRLB) of the channel estimation mean-squared errors.
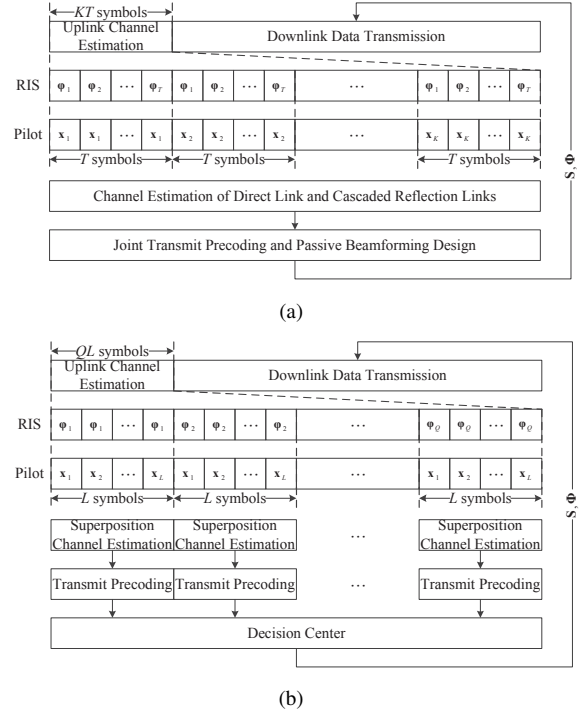

Fig. 2. (a) The frame structure of the DFT-based channel estimation protocol for RIS-assisted MIMO communication systems. (b)The frame structure of the low-complexity channel estimation protocol proposed for RIS-assisted MIMO systems.

This channel estimation protocol and its frame structure are portrayed in Fig. 2(a), where KT TSs are divided into K groups. In each group, the same pilot vector lasts for T TSs. Furthermore, the pilot vectors of the different groups are orthogonal to each other. Specifically, we have $K \geq N_u$ and $T \geq M+1$ for estimating M reflected channels and a single direct channel associated with N_u TAs at the UE. The reflecting elements are always switched on throughout the whole channel estimation phase. In this paper, we consider the case of using the minimum number of pilot symbols, i.e. $K=N_u$ and $T=M+1$. According to the optimal DFT-based configuration scheme of [17], the RIS reflection coefficient of the tth TS is set to $\boldsymbol{\varphi}_t = \mathbf{F}_{t,2:T}^H$, $t=1,\cdots,T$, for an arbitrary pilot vector, where $\mathbf{F} \in \mathbb{C}^{T\times T}$ is the DFT matrix. As a result, for the kth pilot vector, i.e. for the kth group, the received signal of the tth TS at the AP can be expressed as

$$\mathbf{y}_{k,t} = \left[\mathbf{H}_{au}^H + \mathbf{H}_{ar}^H\text{diag}\left(\mathbf{F}_{t,2:T}^T\right)\mathbf{H}_{ru}^H\right]\sqrt{P_{UL}}\mathbf{x}_k + \mathbf{z}_{k,t}$$
$$= \bar{\mathbf{H}}\left(\mathbf{I}_K \otimes \mathbf{F}_{t,:}^T\right)\sqrt{P_{UL}}\mathbf{x}_k + \mathbf{z}_{k,t}, \qquad (4)$$

where $\bar{\mathbf{H}} \in \mathbb{C}^{N_a\times(M+1)N_u}$ contains the channel coefficients of a single direct link and M cascaded AP-RIS-UE links associated with N_u TAs, which is defined by

$$\bar{\mathbf{H}} = \left[\mathbf{H}_{au,1,:}^H, \mathbf{H}_{ar}^H\text{diag}\left\{\mathbf{H}_{ru,1,:}^H\right\}, \cdots,\right.$$
$$\left.\cdots, \mathbf{H}_{au,K,:}^H, \mathbf{H}_{ar}^H\text{diag}\left\{\mathbf{H}_{ru,K,:}^H\right\}\right]. \qquad (5)$$

Let us introduce $\mathbf{Y} = [\mathbf{y}_{1,1},\cdots,\mathbf{y}_{1,T},\cdots,\mathbf{y}_{K,1},\cdots,\mathbf{y}_{K,T}]$, $\mathbf{Z} = [\mathbf{z}_{1,1},\cdots,\mathbf{z}_{1,T},\cdots,\mathbf{z}_{K,1},\cdots,\mathbf{z}_{K,T}]$. Then, upon collecting the signals received within KT TSs, we have

$$\mathbf{Y} = \bar{\mathbf{H}}\mathbf{G} + \mathbf{Z}, \qquad (6)$$

where $\mathbf{G} = \left(\mathbf{I}_K \otimes \mathbf{F}^T\right)\left(\sqrt{P_{UL}}\mathbf{X} \otimes \mathbf{I}_T\right)$ includes both the effect of reflection coefficients at the RIS and that of the pilots transmitted from the UE, i.e., $\mathbf{X} = [\mathbf{x}_1, \cdots, \mathbf{x}_K]$. The orthogonal pilot design of $\mathbf{X}$ follows the conventional MIMO channel estimation techniques [46].

According to (6), the least square (LS) estimate of $\bar{\mathbf{H}}$ can be readily obtained by

$$\hat{\bar{\mathbf{H}}} = \mathbf{Y}\mathbf{G}^H\left(\mathbf{G}\mathbf{G}^H\right)^{-1}. \tag{7}$$

We note that the DFT-based channel estimation method requires at least $(M+1)N_u$ pilot symbols, which is the same as that of the ON/OFF method. Nevertheless, the DFT-based channel estimation method attains the highest accuracy in terms of the channel estimation MSE compared to both the ON/OFF method and to the three-phase method, which is crucial for the optimization of the RIS reflection coefficients.

B. Optimization of the RIS Reflection Coefficients

Based on the estimated CSI, we proceed to design the reflection coefficients at the RIS and transmit precoding at the AP in order to maximize the achievable rate of RIS-assisted MIMO systems in bits per second per Hertz (b/s/Hz) as

$$R = \max_{tr(\mathbf{S}) \leq P_{DL}, \mathbf{S} \succeq \mathbf{0}} \log_2 \det\left(\mathbf{I}_{N_u} + \frac{1}{\sigma_n^2}\mathbf{H}\mathbf{S}\mathbf{H}^H\right). \tag{8}$$

It is worth noting that in contrast to the conventional MIMO channel operating without the RIS, we have $\mathbf{H} = \mathbf{H}_{au}$, where the achievable rate is solely determined by the channel matrix $\mathbf{H}_{au}$ of the direct link, the achievable rate of RIS-assisted MIMO systems shown in (8) is also dependent on the RIS reflection matrix $\mathbf{\Phi}$, since it influences the effective super-imposed channel $\mathbf{H}$ as well as the resultant optimal transmit covariance matrix $\mathbf{S}$. Therefore, maximizing the achievable rate of a RIS-assisted MIMO channel has to jointly optimize the RIS reflection matrix $\mathbf{\Phi}$ and the transmit covariance matrix $\mathbf{S}$, subject to discrete phase shift constraints on the RIS elements and a total power constraint at the AP. Hence, the optimization problem is formulated as:

$$
\begin{aligned}
(P1) \quad \max_{\mathbf{\Phi}, \mathbf{S}} \quad & \log_2 \det\left(\mathbf{I}_{N_u} + \frac{1}{\sigma_n^2}\mathbf{H}\mathbf{S}\mathbf{H}^H\right) \\
s.t. \quad & \mathbf{H} = \mathbf{H}_{au} + \mathbf{H}_{ru}\mathbf{\Phi}\mathbf{H}_{ar}, \\
& \mathbf{\Phi} = \text{diag}\left\{e^{j\theta_1}, \cdots, e^{j\theta_M}\right\}, \\
& \theta_m \in \mathcal{B}, \ m = 1, \cdots, M, \\
& tr\left(\mathbf{S}\right) \leq P_{DL}, \\
& \mathbf{S} \succeq \mathbf{0}.
\end{aligned} \tag{9}
$$

We note that $(P1)$ is a non-convex optimization problem, since the objective function can be shown to be non-concave over the reflection coefficient matrix $\mathbf{\Phi}$, and the discrete phase shift constraint θ_m of each RIS element in (9) is also non-convex. Moreover, the transmit covariance matrix $\mathbf{S}$ is coupled with $\mathbf{\Phi}$ in the objective function of $(P1)$, which makes $(P1)$ more challenging to solve. In [24], the AO algorithm was adopted to solve $(P1)$, where the phase shifts at each RIS element can be flexibly adjusted in $[0, 2\pi]$. More specifically, only a single RIS reflection coefficient is optimized at each step assuming that all the remaining reflection coefficients and $\mathbf{S}$ are given. The optimization of $\mathbf{S}$ given the reflection coefficient matrix $\mathbf{\Phi}$ follows a similar philosophy to that of traditional MIMO systems dispensing with the RIS [47]. Furthermore, we note that the method of [24] can be readily adjusted to solve $(P1)$ by quantizing the estimates of the

RIS reflection coefficient at each step, which constitutes a benchmark scheme for our proposed arrangement.

IV. PROPOSED LOW-COMPLEXITY CHANNEL ESTIMATION AND PASSIVE BEAMFORMING FRAMEWORK

In this section, we will propose a low-complexity channel estimation and passive beamforming design for RIS-assisted MIMO systems. Specifically, the channel estimation protocol of the proposed solution is shown in Fig. 2(b), where the channel training phase is divided into Q training periods, each having a length of L. During each period, the reflection coefficients at the RIS are pre-configured and the effective superimposed channel is estimated instead of separately estimating the direct channel and reflected channels one-by-one. Furthermore, we outline our transmit beamforming design based on the estimated $\mathbf{H}$ in each training period. During each training period, we adjust the reflection coefficients at the RIS and then carry out the channel estimation and transmit beamforming repeatedly. After carrying out both channel estimation and active beamforming Q times, the decision center will compare the objective function value of different training periods and selects the optimum one that maximizes the achievable rate. Hence, the transmit precoding and passive beamforming design are determined accordingly. The detailed procedures of the proposed solution are outlined as follows.

A. Estimation of the Effective Superimposed Channel

The RIS reflection coefficients are generated as shown in Fig. 2(b) for the sake of estimating the effective superimposed channel all-at-once. Let $\mathbf{\Phi}_q, q = 1, \cdots, Q$ denote the RIS reflection coefficient matrix in the qth training period. As a result, the signal received in the lth TS of the qth period can be expressed as

$$
\begin{aligned}
\mathbf{y}_{q,l} &= \left(\mathbf{H}_{au}^H + \mathbf{H}_{ar}^H\mathbf{\Phi}_q^H\mathbf{H}_{ru}^H\right)\sqrt{P_{UL}}\mathbf{x}_l + \mathbf{z}_{q,l} \\
&= \sqrt{P_{UL}}\mathbf{H}_q^H\mathbf{x}_l + \mathbf{z}_{q,l},
\end{aligned} \tag{10}
$$

where $\mathbf{H}_q = \mathbf{H}_{au} + \mathbf{H}_{ru}\mathbf{\Phi}_q\mathbf{H}_{ar}$ denotes the effective super-perposed channel in the qth training period, which combines a single direct channel and M reflected channels in the qth training period; $\mathbf{x}_l, l = 1, \cdots, L$ is the pilot symbol at the lth TS, which is identical for all Q training periods. Following the same considerations as in (4), we assume $L = N_u$ in order to use the minimum number of pilots in each training period.

After collecting L received signals of the qth training period, the signal received by the AP during the qth training period can be expressed as

$$\mathbf{Y}_q = [\mathbf{y}_{q,1}, \cdots, \mathbf{y}_{q,L}] = \sqrt{P_{UL}}\mathbf{H}_q^H\mathbf{X} + \mathbf{Z}_q, \tag{11}$$

where $\mathbf{Z}_q = [\mathbf{z}_{q,1}, \cdots, \mathbf{z}_{q,L}]$ denotes the noise during the qth training period, while $\mathbf{X} = [\mathbf{x}_1, \cdots, \mathbf{x}_L]$ is the pilot matrix used for estimating the effective superposed channel.

As a result, the effective superposed channel estimation of the qth training period is transformed into the classic MIMO channel estimation. It has been shown [46] that the orthogonal pilot design associated with $\mathbf{X}\mathbf{X}^H = \mathbf{I}$ is capable of minimizing the MSE of channel estimates in the MIMO channel estimation. One of the popular practical pilot matrices is constituted by the normalized DFT matrix [46]. Based on the orthogonal pilot design, the LS estimate of the effective

superposed channel $\mathbf{H}_q$ at the qth training period can be expressed as:

$$\hat{\mathbf{H}}_q = \frac{1}{\sqrt{P_{UL}}}\left(\mathbf{X}^H\right)^{-1}\mathbf{Y}_q^H, \tag{12}$$

bearing in mind that we have assumed $L = N_u$ in order to maintain minimum pilot overhead. Nevertheless, (12) can be readily extended to an over-determined system upon replacing the normal inverse by a pseudo-inverse.

It is important to note that the estimate in (12) is the effective superposed channel, which is the superposition of the direct channel and the cascaded reflected channels via the RIS. This is significantly different from prior channel estimation methods designed for RIS-assisted systems.

B. Transmit Precoding Design at the AP

After obtaining the estimates of the effective superposed channel in the qth training period, we proceed to conceive the transmit precoder design at the AP. More specifically given $\hat{\mathbf{H}}_q$, the optimization problem $(P1)$ is reduced to

$$(P2) \quad \max_{\mathbf{S}_q} \quad \log_2 \det\left(\mathbf{I}_{N_u} + \frac{1}{\sigma_n^2}\hat{\mathbf{H}}_q\mathbf{S}_q\hat{\mathbf{H}}_q^H\right)$$
$$s.t. \quad \mathrm{tr}\left(\mathbf{S}_q\right) \le P_{DL}, \tag{13}$$
$$\mathbf{S}_q \succeq \mathbf{0},$$

where $\mathbf{S}_q$ is the transmit covariance matrix in the qth training period.

Note that given the estimated $\hat{\mathbf{H}}_q$, the optimal $\mathbf{S}_q$ follows the singular value decomposition (SVD)-based transmission mode [47], which can be expressed as

$$\hat{\mathbf{S}}_q = \mathbf{V}_q \mathrm{diag}\left\{p_1, \cdots, p_{D_q}\right\}\mathbf{V}_q^H, \tag{14}$$

where $\mathbf{V}_q \in \mathbb{C}^{N_a \times D_q}$ characterizes the truncated SVD of $\hat{\mathbf{H}}_q$, i.e., $\hat{\mathbf{H}}_q = \mathbf{U}_q\mathbf{\Lambda}_q\mathbf{V}_q^H$; D_q denotes the maximum number of data streams that can be transmitted over $\hat{\mathbf{H}}_q$; p_d denotes the optimal water-filling power allocation solution derived for the dth data stream [47]. Hence, given the reflection coefficient matrix $\mathbf{\Phi}_q$, the achievable rate is formulated as:

$$R_q = \sum_{d=1}^{D_q}\log_2\left(1 + \frac{p_d\lambda_d^2}{\sigma_n^2}\right), \tag{15}$$

where λ_d represents the dth diagonal element of $\mathbf{\Lambda}_q$.

C. Optimization of the RIS Reflection Coefficients

Sections IV-A and IV-B describe the effective superposed channel estimation and transmit precoding design given the reflection coefficients at the RIS, which can be readily solved by conventional MIMO techniques designed for operation without the RIS. In this subsection, we will discuss the optimization of the RIS reflection coefficients. More explicitly, in the channel training phase, we invoke different reflection coefficients in different training periods. After performing the effective superposed channel's estimation and transmit precoding Q times, we then select the optimal RIS configuration that maximizes the achievable rate. Once the RIS configuration is obtained, the corresponding effective superposed channel and transmit precoder design are also selected accordingly.

More specifically, the optimization of the RIS reflection coefficients is formulated as:

$$(P3) \quad \max_{q} \quad R_q$$
$$s.t. \quad 1 \le q \le Q. \tag{16}$$

Let $\hat{q}$ denote the optimal index maximizing R_q. Then the optimal reflection coefficient matrix and the transmit covariance matrix can be obtained by $\mathbf{\Phi} = \mathbf{\Phi}_{\hat{q}}$ and $\hat{\mathbf{S}} = \hat{\mathbf{S}}_{\hat{q}}$, respectively.

Remark 1: Recall that in existing RIS-assisted systems, the channel estimation and precoder design are performed only once, as shown in Fig. 2(a). By contrast, the proposed framework has to perform channel estimation and precoder design Q times, as shown in Fig. 2(b). However, the pilot overhead and training complexity of the proposed framework are significantly lower due to the fact that the optimization of RIS reflection coefficients and transmit beamformer are effectively decoupled. This will be shown in Section VI, where our complexity comparison will be elaborated on.

Remark 2: Note that the existing RIS reflection coefficient optimization procedures are generally performed jointly with transmit precoding, which is thus carried out in an iterative manner [12], [24]. By contrast, the proposed scheme first finds the solution set of the RIS reflection coefficient matrix. Following this, we search for the optimal RIS reflection coefficient matrix in the extracted solution set that maximizes the objective function. Therefore, the proposed method does not have to perform multiple iterations, but instead it designs the precoding matrix for each reflection coefficient from the extracted solution set and calculates the resultant objective function value.

Remark 3: In the proposed framework, it is natural to note that the training set of the RIS reflection coefficients has a crucial impact on the achievable rate. For example, if we adopt the same reflection phase configuration for all Q training periods, i.e., $\mathbf{\Phi}_1 = \cdots = \mathbf{\Phi}_Q = \mathbf{\Phi}$, it can be readily seen that the proposed framework becomes equivalent to a random configuration operating without any optimization. Therefore, it is necessary to elaborately design the training set of RIS reflection coefficients for enhancing the system performance, which will be detailed in the next section.

Remark 4: At the time of revising the manuscript, we became aware of another parallel work [29], which also estimates the superimposed channel but focuses on a completely different research topic under the consideration of cell-free massive MIMO systems. Specifically, the authors of [29] configure the RIS by exploiting the statistical knowledge of the CSI, thus each superimposed SISO channel is estimated at each AP only once during the uplink training. Furthermore, spatially correlated fading is also considered in [29]. By contrast, we emphasize that the proposed design first generates a training set for the RIS reflection coefficients and thus performs superimposed MIMO channel estimation and downlink precoding design for each reflection coefficient in the training set. Finally, we choose the best one maximizing/minimizing the objective function value. As a result, the proposed scheme strikes flexible tradeoffs between the pilot overhead and the achievable rate upon adjusting the number of training periods according to the specific QoS requirements

and channel characteristics. More explicitly, we contrast our method to the scheme in [29] in Table II.

V. THE CONFIGURATION METHODS FOR GENERATING THE TRAINING SET OF RIS REFLECTION COEFFICIENTS

In this section, we propose a pair of configuration methods for generating the training set of RIS reflection coefficients over Q training periods, which provides useful insight into the performance characteristics of the proposed framework.

A. Random Configuration

Let us first consider the simple random configuration, where the phase shifts of the RIS elements are randomly generated from the feasible phase shift set in each training period, which can be formulated as

$$\boldsymbol{\theta}_q \sim \mathcal{U}\left(\mathcal{B}^M \Big/ \bigcup_{i=1,\cdots,q-1}\{\boldsymbol{\theta}_i\}\right), \qquad (17)$$

where $\mathcal{B}^M \big/ \bigcup_{i=1,\cdots,q-1} \boldsymbol{\theta}_i$ represents the current phase shift set for the qth training period, and the selected phase shift vectors are removed from the universal set $\mathcal{B}^M$. In fact, although the generation of the training set is offline, it is still not straightforward to generate $\{\boldsymbol{\theta}_1,\cdots,\boldsymbol{\theta}_Q\}$ according to (17), which requires a random number generator with variable seeds. Nonetheless, thanks to the fact that practical RISs are generally equipped with a large number of reflecting elements M, the probability of selecting two identical random phase vectors from B^M candidates in turn is very small, i.e. we have $\lim_{M\to\infty} P\left(\boldsymbol{\theta}_q = \boldsymbol{\theta}_{q'} \,\big|\, \boldsymbol{\theta}_q \in \mathcal{B}^M, \boldsymbol{\theta}_{q'} \in \mathcal{B}^M\right) = 0$. Therefore, we can choose the phase shift vectors directly from $\mathcal{B}^M$ each time without removing the phase shift vector that have been previously selected. As a result, the configuration method of (17) can be reduced to

$$\theta_{m,q} \sim \mathcal{U}\left(\mathcal{B}\right), \ q=1,\cdots,Q, \ m=1,\cdots,M. \qquad (18)$$

To be more explicit, the conflict probability of arbitrary pairs of $(\boldsymbol{\theta}_q, \boldsymbol{\theta}_{q'})$ from a Q-entry training set generated by (18), namely, the probability that at least two of the elements in the training set are the same, is given by

$$P_c = 1 - \frac{C_{B^M}^Q Q!}{(B^M)^Q} = 1 - \frac{(B^M)!}{B^{QM}(B^M - Q)!}, \qquad (19)$$

where $C_{B^M}^Q Q!$ denotes the number of training sets having Q distinct elements, while $(B^M)^Q$ represents the number of possible training sets given Q. For example, if we consider a RIS with $M = 50$ reflecting elements, each with $B = 2$ possible phase shifts, the conflict probability of arbitrary pairs of $(\boldsymbol{\theta}_q, \boldsymbol{\theta}_{q'})$ from the training set generated by (18) is $P_c \approx 4 \times 10^{-14}$ for $Q = 10$. It is clear that further increasing the number of reflecting elements M will lead to a diminishing conflict probability, which is difficult to calculate even by numerical methods. More explicitly, we plot the conflict probability under different M in Fig. 3. It can be seen that the conflict probability is a very small value under moderate Q and will further decrease with M, which implies that there are almost no identical elements in the extracted Q-entry training set based on (18). As a result, the random configuration according to (18) incurs almost no performance penalty compared to (17).
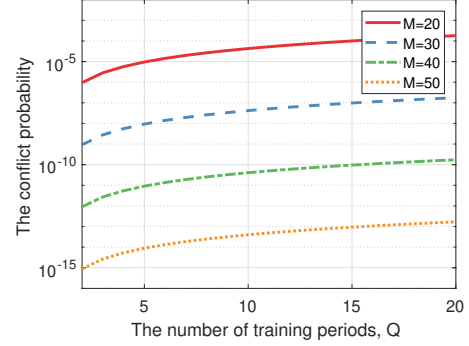

Fig. 3. The conflict probability caused by the simplified random configuration.

Next, we will analyze the scaling law of the average power received at the UE for characterizing the performance of the proposed framework having random configuration. Before we start, we first give *Lemma 1* formulated from the conclusions of [48], which provides useful support for our theoretical analysis.

Lemma 1: For n independent random samples from an exponential distribution with parameter λ, the order statistics $\alpha_{(i)}$ for $i = 1, 2, \ldots, n$ have the following distribution

$$\alpha_{(i)} \stackrel{d}{=} \frac{1}{\lambda}\left(\sum_{j=1}^{i}\frac{\beta_j}{n-j+1}\right), \qquad (20)$$

where β_j are i.i.d. standard exponential random variables with a rate parameter of 1.

Furthermore, for the sake of simplicity, let us firstly consider the case of $N_a = N_u = 1$ in order to gain essential insights. Moreover, we assume that the direct link equals zero since the reflected links become more dominant than the direct link as $M \to \infty$. As a result, the average power P_r received at the UE using the proposed framework having random configuration is given by

$$P_r = P_{DL}\mathbb{E}\left\{\max_{q=1,\cdots,Q}\left\{\left|\sum_{m=1}^{M} h_{ar,m}\varphi_{m,q}h_{ru,m}\right|^2\right\}\right\}, \qquad (21)$$

where P_{DL} is the transmit power of the AP, while $\mathbf{h}_{ar} = [h_{ar,1},\cdots,h_{ar,M}]^T$ and $\mathbf{h}_{ru} = [h_{ru,1},\cdots,h_{ru,M}]$ represent the degradation of $\mathbf{H}_{ar}$ and $\mathbf{H}_{ru}$, respectively. We assume having i.i.d. Rician fading with average powers of ρ_{ar}^2 and ρ_{ru}^2 for each entry in $\mathbf{h}_{ar}$ and $\mathbf{h}_{ru}$, respectively. Specifically, let $h_{ar,m} = \rho_{ar}\left(\sqrt{K_{ar}/(K_{ar}+1)}h_{ar,m}^{LoS} + \sqrt{1/(K_{ar}+1)}h_{ar,m}^{NLoS}\right)$ and $h_{ru,m} = \rho_{ru}\left(\sqrt{K_{ru}/(K_{ru}+1)}h_{ru,m}^{LoS} + \sqrt{1/(K_{ru}+1)}h_{ru,m}^{NLoS}\right)$ denote the channel model of the AP-RIS and RIS-UE link, respectively, where $K_{ar} \geq 0$, $\left|h_{ar,m}^{LoS}\right| = 1$, $h_{ar,m}^{NLoS} \sim \mathcal{CN}(0,1)$ denote the Rician factor, the deterministic LoS component, and the complex Gaussian-distributed NLoS component, respectively, for the AP-RIS link. Furthermore, $K_{ru} \geq 0$, $\left|h_{ru,m}^{LoS}\right| = 1$, $h_{ru,m}^{NLoS} \sim \mathcal{CN}(0,1)$ denote the Rician factor, the deterministic LoS component, and the complex Gaussian-distributed NLoS component, respectively, for the RIS-UE link. Based on this assumption, the average power received at the UE of the proposed framework having

TABLE II
THE CONTRAST OF THE PROPOSED METHOD TO THE SCHEME IN [29].

		The proposed method	The method in [29]
Similarity		Estimation of the superimposed end-to-end channel	
D i f f e r e n c e	Setup	Single-user MIMO	Cell-free massive MIMO
	Operation	1. Generates the training set of RIS reflection coefficients off-line; 2. Estimates the superimposed channel and performs the transmit precoding design for each RIS reflection coefficients; 3. Selects the best one.	1. Performs the RIS configuration based on the statistical CSI; 2. Estimates the superimposed channel and performs the transmit precoding design.
	Objective function for RIS configuration	Flexible, depends on the specific requirements	Fixed, the sum of NMSEs of channel estimates
	Statistical CSI	Not required	Required
	Pilot overhead	Adjustable	Fixed, minimum
	Rate performance	Suffers from performance loss in slow time-varying channel fadings	Depends on the bias between the real channel and the channel statisticals
	Application scope	Arbitrary channel modelling	Slow time-varying channels having accurate channel statisticals

random configuration for the RIS-assisted SISO systems is summarized in *Proposition 1*.

Proposition 1: Upon assuming i.i.d. Rician fading with average powers of ρ_{ar}^2 and ρ_{ru}^2 for each entry of $h_{ar,m}$ and $h_{ru,m}$, respectively, as $M \to \infty$, it holds that

$$P_r \to P_{DL} \rho_{ar}^2 \rho_{ru}^2 M \left(\log Q + C \right), \qquad (22)$$

where $C \approx 0.57722\ldots$ is the Euler-Mascheroni constant [49].

Proof: For a single random RIS configuration, based on the Lindeberg-Levy central limit theorem [12], we have $\omega_q = \sum_{m=1}^{M} h_{ar,m} \varphi_{m,q} h_{ru,m} \sim \mathcal{CN}\left(0, M\rho_{ar}^2\rho_{ru}^2\right)$ as $M \to \infty$. Note that this distribution approximation is independent of the Rician factor of the AP-RIS and of the RIS-UE links since we have $\theta_{m,q} = \angle \varphi_{m,q} \sim \mathcal{U}\left(\mathcal{B}\right)$. According to *Lemma 1*, the distribution of the Qth order statistics $\max_{q=1,\cdots,Q}\left\{|\omega_q|^2\right\}$ is thus given by

$$\max_{q=1,\cdots,Q}\left\{|\omega_q|^2\right\} \stackrel{d}{=} M\rho_{ar}^2\rho_{ru}^2 \sum_{j=1}^{Q} \frac{1}{Q-j+1}\beta_j. \qquad (23)$$

As a result, the expectation of the Qth order statistics $\max_{q=1,\cdots,Q}\left\{|\omega_q|^2\right\}$ can be obtained by

$$\mathbb{E}\left\{\max_{q=1,\cdots,Q}\left\{|\omega_q|^2\right\}\right\} = \mathbb{E}\left\{M\rho_{ar}^2\rho_{ru}^2 \sum_{j=1}^{Q} \frac{1}{Q-j+1}\beta_j\right\}$$

$$\stackrel{(a)}{=} M\rho_{ar}^2\rho_{ru}^2 \sum_{j=1}^{Q} \frac{1}{Q-j+1}$$

$$\stackrel{Q\to\infty}{=} M\rho_{ar}^2\rho_{ru}^2\left(\log Q + C\right), \qquad (24)$$

where (a) holds due to $\mathbb{E}\left\{\beta_j\right\} = 1$, $j = 1,\cdots,Q$. Upon substituting (24) into (21), the proof is completed. ∎

Proposition 1 reveals the power scaling law of the proposed framework. Note that here we use the general formula of $\sum_{j=1}^{Q} \frac{1}{Q-j+1} \stackrel{Q\to\infty}{=} \log Q + C$ for the sake of explicitly characterizing the relationship of P_r versus Q. In fact, for a small value of Q, we could calculate $\sum_{j=1}^{Q} \frac{1}{Q-j+1}$ numerically to obtain a more accurate theoretical P_r. Furthermore, the performance of the proposed scheme is independent of the number of quantization bits, which is different from the existing solutions of [12]. Hence, the proposed solution is more suitable for a RIS relying on one-bit quantized phase shifts, which will be verified by our simulations. Moreover, the appearance of $\log(Q)$ in (21) makes it possible to strike a flexible balance between the pilot overhead and the system

performance. More specifically, when the number of training periods is $Q = 1$, we strictly have $P_r = MP_{DL}\rho_{ar}^2\rho_{ru}^2$, which is equivalent to the single random configuration. Furthermore, as $Q \to \infty$, we have a quadratic scaling law vs. M, i.e., $P_r \to M^2 P_{DL}\rho_{ar}^2\rho_{ru}^2 \log B$, where the maximum number of training periods $Q_{\max} = B^M$ is considered. More specifically, our performance comparison between the proposed framework and the optimal RIS configuration derived for moderate Q is summarized in *Corollary 1*.

Corollary 1: Assuming that $h_{ar,m} \sim \mathcal{CN}\left(0, \rho_{ar}^2\right)$, $h_{ru,m} \sim \mathcal{CN}\left(0, \rho_{ru}^2\right)$, $m = 1, \cdots, M$. For a large M, it holds that[2]

$$\frac{P_r}{P_{r,optimal}} \propto \frac{16\left(\log Q + C\right)}{\pi^2 M}, \qquad (25)$$

where $P_{r,optimal} \to P_{DL}\rho_{ar}^2\rho_{ru}^2 M^2 \pi^2 / 16$ is the average power received at the UE for the optimal RIS configuration [12].

It can be seen from *Corollary 1* that the proposed framework using random RIS configuration has a slight power loss compared to the optimal RIS configuration, which can be compensated by increasing the number of training periods. Additionally, the proposed framework is more robust to channel estimation errors, and thus the performance gap can be further narrowed for the practical cases associated with imperfect CSI, which will be verified by our simulations.

B. Euclidean Distance Maximizing Configuration

In the proposed framework, our main objective is to design the best reflection coefficient vectors. It is plausible that the random configuration does not exploit the Q training periods efficiently. Explicitly, the random configuration may generate some RIS reflection coefficients that are similar to each other, which may result in similar system performance. Therefore, we propose a more sophisticated configuration of the RIS reflection coefficients based on the following heuristic philosophy: the more different the RIS reflection coefficients are, the more different the channels generated, thus leading to Q candidates with significant differences. In this paper, we use the sum of Euclidean distances of all pairs of RIS reflection coefficients to characterize this difference. Therefore, the optimization problem of the reflection coefficients can be expressed as

$$(P4) \quad \max_{\boldsymbol{\varphi}_1,\cdots,\boldsymbol{\varphi}_Q} \quad \sum_{q=1}^{Q} \sum_{q'=1,q'\neq q}^{Q} \left\|\boldsymbol{\varphi}_q - \boldsymbol{\varphi}_{q'}\right\|^2 \qquad (26)$$
$$s.t. \quad \boldsymbol{\varphi}_q = e^{j\boldsymbol{\theta}_q}, \boldsymbol{\theta}_q \in \mathcal{B}^M.$$

---

[2]Note that here we consider Rayleigh fading in order to maintain the same assumption as in [12].

TABLE III
THE EUCLIDEAN DISTANCE MAXIMIZING CONFIGURATION FOR
GENERATING THE TRAINING SET OF RIS REFLECTION COEFFICIENTS

1: Randomly generate a training set of RIS reflection coefficients,
   e.g., $\varphi_1, \cdots, \varphi_Q$;
2: Calculate $\eta_q = \sum_{q'=1, q'=q}^{Q} \left\| \varphi_q - \varphi_{q'} \right\|^2$ for each φ_q;
3: Initialization of the counter, $i = 0$;
4: **while** $i < Q_{new}$
5:    Find the minimum value $\eta_{\min}$ from $\{\eta_1, \cdots, \eta_Q\}$ and the
      corresponding φ_m;
6:    Randomly generate new reflection coefficients, φ';
7:    Calculate $\eta' = \sum_{q=1}^{Q} \left\| \varphi' - \varphi_q \right\|^2$ for φ';
8:    **if** $\eta' > \eta_{\min}$
9:      $\varphi_m \leftarrow \varphi'$, $i \leftarrow i + 1$;
10:   **end**
11: **end**
12: **Output:** $\varphi_1, \cdots, \varphi_Q$.

We note that it is not trivial to find the optimal phase shift set of (26), because we have to search through $C_{B^M}^Q$ possible phase shift candidates, which is excessive in practical implementations. To solve this problem, we propose an ad hoc method for asymptotically finding the optimal solution of $(P4)$. Specifically, we first randomly generate a phase shift set $\{\varphi_1, \cdots, \varphi_Q\}$ following the above random configuration, and then we calculate the metrics $\eta_q = \sum_{q'=1, q'=q}^{Q} \left\| \varphi_q - \varphi_{q'} \right\|^2$ for each phase shift vector φ_q. Next, we randomly generate new phase shift vectors from $\mathcal{B}^M$ to replace the phase shift vectors having smaller η_q, until $\sum_{q=1}^{Q} \sum_{q'=1, q' \neq q}^{Q} \left\| \varphi_q - \varphi_{q'} \right\|^2$ in (26) is close to convergence. More specifically, the detailed steps are described in Table III. For the sake of efficiency, we use a maximum number Q_{new} of iterations instead of the convergence condition of Table III. In our simulations, we set $Q_{new} = 5Q$ by default.

Additionally, although we consider discrete phase shifts in this paper, the proposed method can be readily extended to the case of having RISs with continuous phase shifts. Specifically, we only have to adapt the training set of RIS reflection coefficients for the continuous phase shifts. For the detailed configuration method of generating the training set of continuous phase shifts, please refer to our extended technical report [50].

VI. ADVANTAGES OF THE PROPOSED FRAMEWORK

In this section, we will discuss the advantages of the proposed low-complexity framework over its counterparts, which can be summarized from the following four aspects:

A. Simplified System Complexity

As stated earlier, both the channel estimation and transmit precoding of the RIS-assisted systems are coupled with the optimization of RIS reflection coefficients, which imposes challenges on their practical implementation. By contrast, the proposed framework significantly simplifies the complex signal processing problems of the existing solutions.

More specifically, the conventional channel estimators of RIS-assisted MIMO systems have to estimate a single direct channel and M reflected channels, which has the complexity of $C_{CE,AO} = 2N_a N_u (M + 1)$ in terms of the number of real-valued multiplications [17]. By contrast, the proposed solution only estimates a single effective superposed channel in each training period. Hence, its complexity is $C_{CE,Pro} = 2N_a N_u Q$, where $Q \geq 1$ can be flexibly chosen based on the specific QoS requirements. In terms of the transmit precoder design and passive beamforming, the complexity is non-trivial to assess explicitly due to the complex optimization involved, and thus we adopt the complexity order to characterize the computational complexity of passive beamforming. Assuming that the AO algorithm is applied for solving $(P1)$, the complexity order is $C_{PB,AO} = \mathcal{O}\left[N_i \left(N_a^3 + BM \left(MN_aN_u + N_aN_u^2 + N_u!\right)\right)\right]$, where N_i represents the number of iterations in the AO algorithm, while $\mathcal{O}\left(N_a^3\right)$ quantifies the complexity order of performing SVD-based transmission at the transmitter; Furthermore, $\mathcal{O}\left(MN_aN_u\right)$, $\mathcal{O}\left(N_aN_u^2\right)$, and $\mathcal{O}\left(N_u!\right)$ signify the complexity order of calculating $\mathbf{H}_{ru}\mathbf{\Phi}\mathbf{H}_{ar}$, $\mathbf{HSH}^H$, and R, respectively [24]; BM represents the number of feasible candidates for optimizing the phase shift at each RIS element one-by-one. By contrast, in the proposed algorithm, only the optimization of the transmit covariance matrix and the calculation of the resultant achievable rate has to be completed during each period at a complexity order of $C_{PB,Pro} = \mathcal{O}\left[Q\left(N_a^3 + N_aN_u^2 + N_u!\right)\right]$. This significantly alleviates the computing burden.

B. Flexible Protocol Design

In contrast to the existing solutions, the proposed framework can strike a flexible performance vs. the pilot overhead trade-off. More specifically, the pilot overhead of the simplest ON/OFF method [16] and of the DFT-based method is $(M + 1)N_u$ [17]. Although the three-phase method and the grouping-based method reduce the pilot overhead, this is achieved at the cost of a performance penalty [19], [21]. Furthermore, the pilot overhead of these methods is still dependent on the number of reflecting elements M. By contrast, the proposed framework has a reduced pilot overhead of QN_u, which is independent of the number of RIS elements and thus can be dynamically adjusted to strike a flexible trade-off between the system performance and the pilot overhead.

C. Reduced Backhaul Consumption

In the existing RIS-assisted communication systems, the optimization of the reflection coefficients is performed at the control center. As a result, the system requires extra backhaul capacity for feeding back Mb bits to the RIS through the control link, which is a challenge for practical RISs having a large number of reflecting elements. By contrast, in our proposed framework, the RIS configuration can be performed by feeding back only the index of the optimal training period to the RIS, hence the number of signaling bits is $\lceil \log_2 Q \rceil$. It is noted that the control signaling requirement of the proposed framework is independent of the number of quantization bits of the phase shifts and of the number of the RIS elements,

hence the index of the optimal training period is sufficient for the RIS configuration, regardless of whether the full- or limited-precision RIS reflecting elements are considered. It is plausible that the proposed framework significantly reduces both the backhaul requirement and the transmission delay between the control center and the RIS compared to the traditional framework.

D. Channel Model Independent

Compared to the existing RIS-aided communication protocols of [19]–[24], [28], [29], the proposed method does not depend on the specific model of the channel reflected by the RIS. At each training period, only the reflection coefficients have to be configured and the AP will estimate the superimposed MIMO channel. By contrast, in the existing schemes, the cascaded AP-RIS-UE channels are estimated, and the channel estimation algorithms generally have to consider, for example, the spatial correlation between different reflected channels [21], [28], [29]. Alternatively, they exploit the similarity of the AP-RIS link between different antennas [19] or alternatively the sparsity of the AP-RIS link [20]. By contrast, the proposed method reduces the dependence on the specific channel model and thus has a wider range of applications than the existing RIS-aided communication protocols of [19]–[24], [28], [29].

VII. SIMULATION RESULTS

In this section, we will evaluate the achievable rate of the proposed framework by considering a three-dimensional Cartesian coordinate system. We assume that both the AP and the UE are equipped with a uniform linear array located on the y-axis with an antenna spacing of $d_A = \lambda/2$, where λ denotes the wavelength. More specifically, the number of antennas at the AP and UE are set to $N_a = 8$ and $N_u = 4$, respectively. Furthermore, the RIS relying on a uniform rectangular array is deployed on the $x - z$ plane for enhancing the MIMO transmissions using a RIS element spacing of $d_I = \lambda/2$ and a fixed number of $M_x = 10$ elements on the x-axis. Unless specified otherwise, we consider single-bit quantization for the phase shifts at each reflecting element, i.e, $\mathcal{B} = \{0, \pi\}$, which is the most common design in practical implementations. The locations of the reference antenna/element at the AP, the RIS, and the UE are set to $(0,0,0)$, $(d_0,0,0)$ and $(d,d_v,0)$, respectively, whose relative positions are illustrated in Fig. 4. As a result, the lengths of the AP-UE link, the AP-RIS link, and the RIS-UE link can be obtained as $d_{au} = \sqrt{d^2 + d_v^2}$, $d_{ar} = d_0$, and $d_{ru} = \sqrt{d_v^2 + (d_0 - d)^2}$, respectively. In our simulations, we set the horizontal distance from the AP to the RIS and the vertical distance between the AP-RIS line and UE line as $d_0 = 50$ m and $d_v = 5$ m, respectively, since the RIS is deployed near the UE to improve its performance [5].

Moreover, we consider narrowband MIMO communications and adopt the Rician fading model for all the channels, $\mathbf{H}_{au}$, $\mathbf{H}_{ar}$, and $\mathbf{H}_{ru}$. For an arbitrary $\mathbf{H} \in \{\mathbf{H}_{au}, \mathbf{H}_{ar}, \mathbf{H}_{ru}\}$, the channel matrix $\mathbf{H}$ is modeled as [12]:

$$\mathbf{H} = \sqrt{\frac{C_0 d^{-\alpha}}{K+1}} \left(\sqrt{K}\mathbf{H}_{LoS} + \mathbf{H}_{NLoS} \right), \quad (27)$$
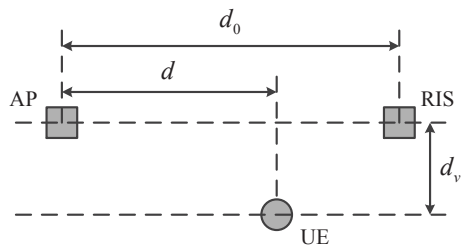

Fig. 4. The relative positions of the AP, RIS and UE (top view).

where $\mathbf{H}_{LoS}$ and $\mathbf{H}_{NLoS}$ denote the LoS component and the NLoS component, respectively; while d, α and K denote the transmission distances, the path loss exponents and Rician factors, respectively, of the corresponding link. Note that by considering different K values, this model corresponds to various practical channels including the deterministic LoS channel as $K \to \infty$, and the Rayleigh fading channel when $K = 0$. In our simulations, the Rician factors of the AP-RIS channel $\mathbf{H}_{ar}$ and the RIS-UE channel $\mathbf{H}_{ru}$ are set to $K_{ar} = 5$ dB and $K_{ru} = 3$ dB, respectively, since the RISs are generally positioned for facilitating LoS propagation for both the AP-RIS link and the RIS-UE link. The direct link is modelled by (27) using a Rician factor of $K_{au} = 0$. Furthermore, $C_0 d^{-\alpha}$ characterizes the distance-dependent large-scale fading for all channels, where $C_0 = -20$ dB denotes the path loss at the reference distance of 1 m. The path loss exponents for the AP-UE, AP-RIS and RIS-UE links are set as $\alpha_{au} = 3.5$, $\alpha_{ar} = 2.2$, and $\alpha_{ru} = 2.8$, respectively [24]. Moreover, we set the transmit power constraint of $P_{DL} = 20$ dBm for the downlink transmission considered, while the average noise power of the narrowband MIMO systems is set to $\sigma_n^2 = -70$ dBm. All the results are averaged over 1000 independent channel realizations. To start with, several benchmark schemes and their simulation settings are listed as follows:

1) Without RIS: Maximizing the achievable rate in (8) by optimizing $\mathbf{S}$ using $\mathbf{H} = \mathbf{H}_{au}$;

2) Random phase shift: Randomly generate $\{\theta_1, \cdots, \theta_M\}$ with $\theta_m \in \mathcal{B}$, $m = 1, \cdots, M$. Maximizing the achievable rate in (8) by optimizing $\mathbf{S}$ using $\mathbf{H} = \mathbf{H}_{au} + \mathbf{H}_{ru}\mathbf{\Phi}\mathbf{H}_{ar}$;

3) Alternating optimization[3]: Alternately optimizing $\mathbf{\Phi}$ and $\mathbf{S}$ according to the closed-form solutions in [24]. The phase shift obtained at each step is quantized into $\mathcal{B}$ based on the minimum Euclidean distance. The convergence threshold in terms of the relative increment in the achievable rate is set to $\varepsilon = 10^{-3}$.

Additionally, for each scenario, we will consider the cases of perfect and imperfect CSI, respectively. More specifically, when considering practical channel estimation, the uplink average pilot power is set to $P_{UL} = 0$ dBm, and the average

[3]When considering the effect of the practical channel estimates, the AO algorithm in [24] needs to know $\mathbf{H}_{au}, \mathbf{H}_{ar}, \mathbf{H}_{ru}$. Unfortunately, it is difficult for the aforementioned cascade channel estimation schemes to obtain separate $\mathbf{H}_{ar}$ and $\mathbf{H}_{ru}$. Therefore, we have to design a semi-passive channel estimator for the AO algorithm of [24], namely, the RIS can operate in the channel sensing mode by activating the sensors to receive pilots from AP/UE, while turning off all the reflecting elements [10]. By contrast, the RIS in our systems is completely passive. Hence, this is actually an unfair comparison strategy for our proposed scheme.
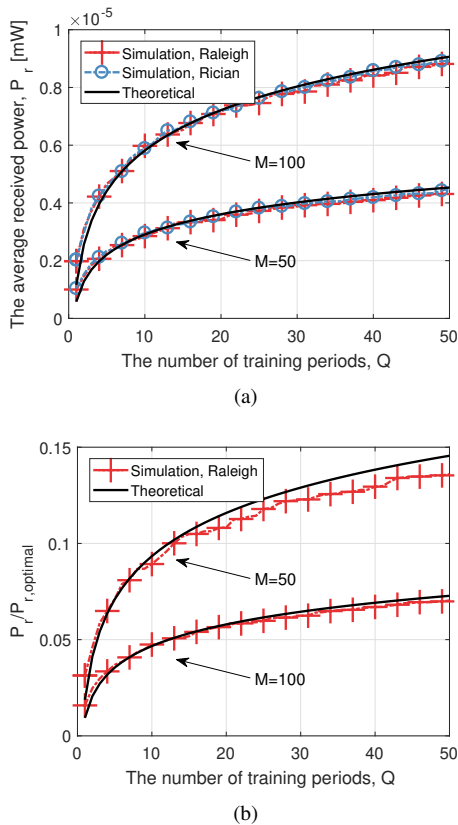
Fig. 5. (a) The average received power under different channel models for SISO scenario. (b) The average received power comparison of the proposed scheme and the optimal configuration.

noise power at the AP is set to $\sigma_z^2 = -60$ dBm. Furthermore, the ergodic achievable rate is given by

$$R_{\text{imperfect CSI}} = \mathbb{E}\left\{ \log_2 \det\left(\mathbf{I}_{N_u} + \frac{1}{\sigma_n^2} \mathbf{HSH}^H \right) \right\}, \qquad (28)$$

where $\mathbf{S}$ is designed based on the estimated $\mathbf{H}$. The ergodic achievable rate with imperfect CSI in (28) is totally different from the expected achievable rate in (13), where the estimated $\mathbf{H}$ is employed instead for the optimization of $\mathbf{S}$. Note that (28) actually describes the ergodic achievable rate in a slow time-varying channel, where the effect of pilot overhead is ignored. We only consider the AO algorithm since it remains the optimal performance in the slow time-varying channels. The comparison of the proposed scheme with other recent methods will be detailed under the fast time-varying channels later.

First of all, we verify our theoretical analysis by considering $N_a = N_u = 1$ and assuming that the direct link is blocked. The corresponding simulation results are shown in Fig. 5(a), where Rayleigh fading and Rician fading correspond to $K_{ar} = K_{ru} = 0$ and $K_{ar} = 5$ dB, $K_{ru} = 3$ dB, respectively. It can be seen from Fig. 5(a) that the performance of the proposed algorithm increases logarithmically with the number of training periods Q, regardless of the fading distribution, which once again confirms the independence of the proposed scheme of the specific channel model. Moreover, the theoretical results in *Proposition 1* perfectly characterize the system performance under all setups. Furthermore, Fig. 5(b) compares the average

received power of the proposed scheme to that associated with the optimal RIS configuration. It can be seen that the proposed algorithm suffers from some performance erosion compared to the optimal configuration, but has a range of other benefits, as demonstrated in Section V. Additionally, the performance gap can be bridged by increasing the number of training periods. Moreover, it can be observed that for a given Q, the performance loss is more severe for a large M, which implies that for a large RIS array, more training periods are required for improving the system performance. In contrast to the schemes where the pilot overhead is proportional to M, the proposed arrangement can flexibly adjust the training period for striking tradeoffs between the pilot overhead imposed and the performance attained.

Next, let us consider the scenario that the UE moves around the RIS, where the number of reflecting elements is set to $M = 50$. More specifically, the horizontal distance between the UE and AP gradually increases from $d = 25$ m to $d = 75$ m. The simulation results with perfect CSI and imperfect CSI are shown in Fig. 6(a) and Fig. 6(b), respectively. We use the acronyms 'RC' and 'EMC' in the legends of Figs. 6(a) $\sim$ 6(b) to represent the proposed random configuration and Euclidean distance maximizing configuration, where the number of training periods is set to $Q = 50$. Observe from Fig. 6(a) that the RIS significantly increases the achievable rate of UEs in its vicinity compared to the case in the absence of the RIS. Additionally, compared to the random phase shift setting, both the proposed framework and the AO algorithm attain considerable performance improvement. Furthermore, compared to the optimal AO algorithm, our proposed schemes have only about 1b/s/Hz performance penalty during the whole UE movement process, despite avoiding the complex alternating optimization process and the acquisition of CSI. Furthermore, when considering the practical scenarios having imperfect CSI, as shown in Fig. 6(b), the proposed framework has a higher rate than the AO algorithm, despite its lower complexity.

Figs. 7(a) $\sim$ 7(b) portray the achievable rate of different schemes versus the number of training periods, which correspond to the case without/with channel estimation errors, respectively. The UE's horizontal distance from the AP is fixed at $d = 50$ m, while the number of reflecting elements follows the setting of Fig. 6(a). Observe from Fig. 7(a) that the achievable rate of the proposed solution increases with the number of training periods, which is not the case for its existing counterparts. In particular, when $Q = 1$, the proposed algorithm is equivalent to a single random configuration, while when $Q \to \infty$, the proposed algorithm will gradually approach the maximal achievable rate. However, its convergence will slow down upon increasing of Q, which is consistent with *Proposition 1*, namely that we have $R \propto \log\left[\log\left(Q\right)\right]$ for high SNRs. Furthermore, the improved configuration method of generating the training set has a faster convergence than the random configuration. For example, for the Euclidean distance maximizing configuration method, it requires only $Q = 10$ training periods to reach the rate of 25 b/s/Hz, while at least $Q = 50$ training periods are required upon using the random configuration. Furthermore, when considering prac-
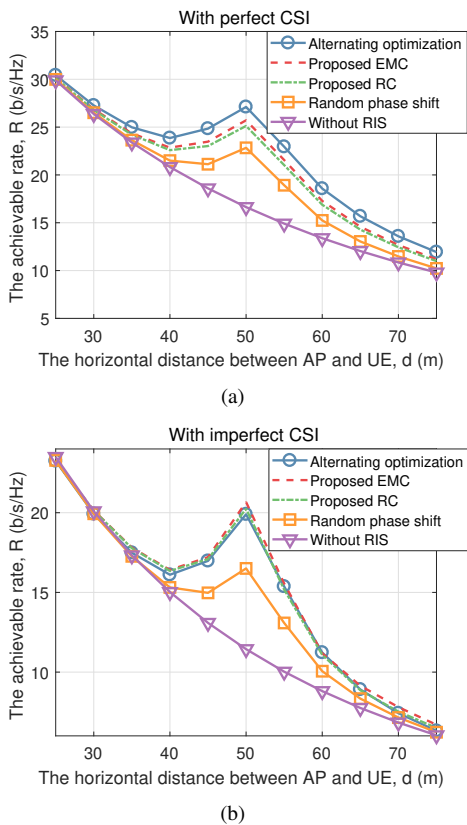
(a)

(b)

Fig. 6. (a) The achievable rate versus the horizontal AP-UE distance with perfect CSI. (b) The achievable rate versus the horizontal AP-UE distance with imperfect CSI.
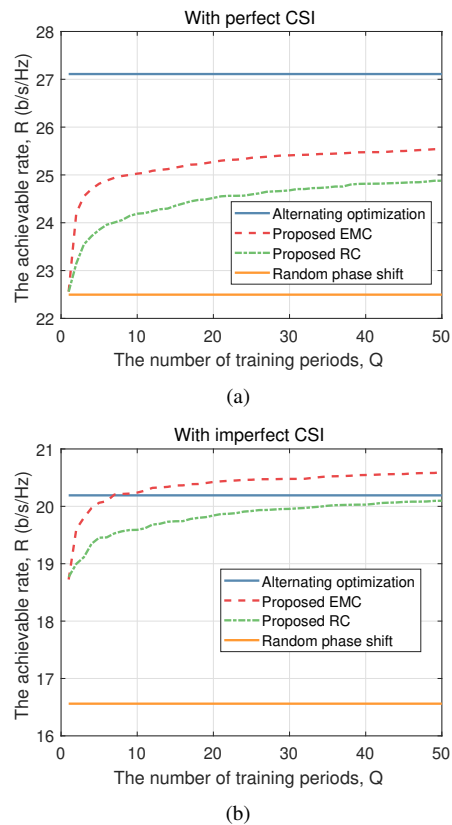

(a)

(b)

Fig. 7. (a) The achievable rate versus the number of training periods with perfect CSI. (b) The achievable rate versus the number of training periods with imperfect CSI.

tical channel estimation errors, Fig. 7(b) demonstrates that the proposed scheme relying on the improved configuration method outperforms even the AO algorithm when $Q > 10$, indicating that the AO algorithm is more sensitive to the channel estimation errors.

Next, the achievable rate versus the number of reflecting elements is shown in Figs. 8(a) $\sim$ 8(b), where the number of training periods is set to $Q = 50$. Observe that compared to the AO algorithm, the proposed algorithm has a slight advantage for a low number of reflecting elements. More specifically, under perfect CSI, the proposed algorithm performs better for a low number of reflecting elements, such as $M \leq 20$. When the channel estimation error is taken into account, Fig. 8(b) shows that the proposed algorithm extends these rate advantages to a moderate number of reflecting elements, such as $M \leq 70$. The performance advantage will become more significant with the increase of the channel estimation error. This is because the proposed algorithm can search through almost the entire discrete solution space for the low number of reflecting elements, but the AO algorithm can only ensure convergence to a locally optimal solution. Additionally, when there is no channel estimation error, the rate of the proposed algorithm grows according to $R \propto \log(M)$, which is a factor two slower than that of the AO algorithm given by $R \propto 2\log(M)$. However, this rate difference can be compensated by increasing the number of training periods. When considering practical systems having realistic channel

estimation errors, the performance loss can also be alleviated, as shown in Fig. 8(b).

Furthermore, we study the effect of the RIS phase shift levels on the achievable rate of the proposed solution. Likewise, Fig. 9(a) and Fig. 9(b) represent the cases associated with perfect CSI and imperfect CSI, respectively. The number of reflecting elements is set to $M = 50$, while the number of training periods is set to $Q = 50$ and the number of quantization bits increases from $b = 1$ to $b = 5$. It can be seen from Figs. 9(a) $\sim$ 9(b) that only the performance of the AO algorithm improves upon increasing the number of quantization bits, while the performance of the proposed algorithm and the random phase shift is robust to the quantization errors, which is consistent with *Proposition 1*. Therefore, the proposed scheme is more suitable for using low-precision phase shifts at the RIS, which is easy to design in practical implementations. In particular, when considering the effects of channel estimation errors, as shown in Fig. 9(b), the proposed scheme employing the one-bit quantized phase shifts is more competitive than the AO algorithm, which once again verifies the conclusions of our prior simulation results.

Recently, some novel channel estimation and passive beamforming methods were proposed for reducing both the pilot overhead and the complexity. Next, we will compare our methods to some of these recent counterparts upon considering rapidly time-varying channels. Since the number of pilots and other parameters required for passive beamforming in these methods are generally different, the achievable rate is
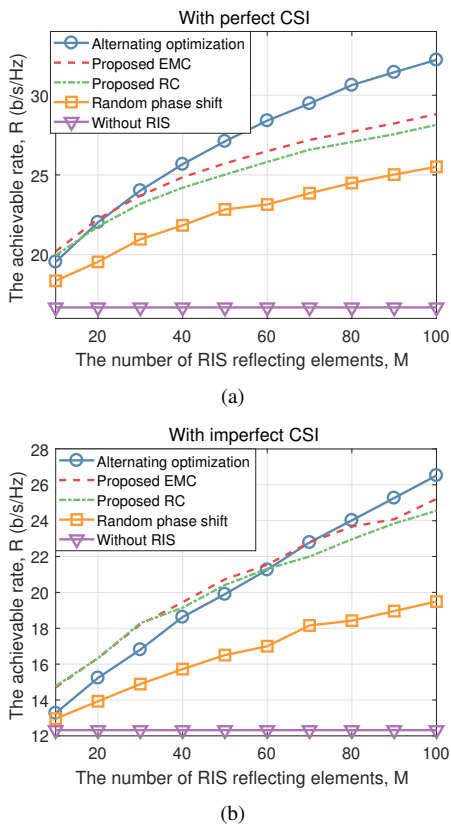
(a)

(b)

Fig. 8. (a) The achievable rate versus the number of RIS reflecting elements with perfect CSI. (b) The achievable rate versus the number of RIS reflecting elements with imperfect CSI.
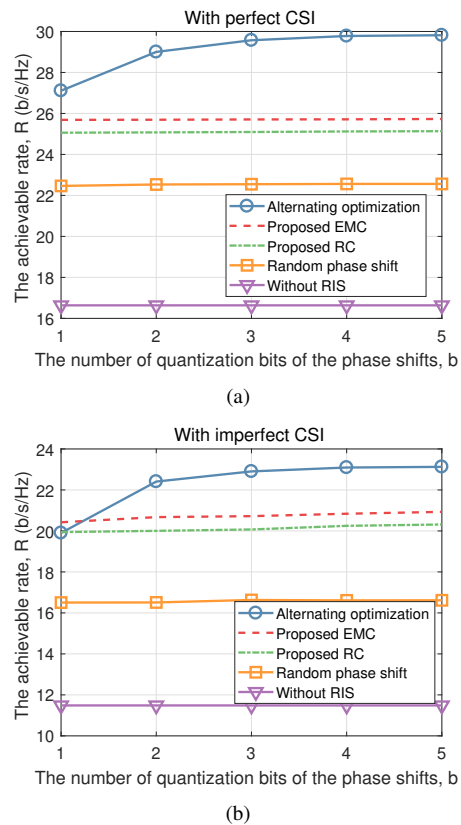

(a)

(b)

Fig. 9. (a) The achievable rate versus the quantization bits of phase shifts with perfect CSI. (b) The achievable rate versus the quantization bits of phase shifts with imperfect CSI.

employed as our metric, which comprehensively considers the influence of both the channel estimation and passive beamforming. Specifically, the effective achievable rate is defined as follows:

$$R_e = \frac{T - \tau}{T} \mathbb{E} \left\{ \log_2 \det \left(\mathbf{I}_{N_u} + \frac{1}{\sigma_n^2} \mathbf{H} \mathbf{S} \mathbf{H}^H \right) \right\}, \quad (29)$$

where T represents the channel's coherence time interval and τ is the pilot overhead, both in terms of the number of symbols. Additionally, we consider the following schemes: (1) *Statistical CSI-based scheme:* completes the RIS configuration based on the statistical CSI and thus carries out end-to-end superimposed channel estimation as well as the ensuing transmit beamforming design [27], [29]; (2) *Grouping-based scheme:* arrange the RIS elements into groups and then estimates only a common reflected channel for each group and uses the same reflection coefficient for each coefficient within the group [21]. It is important to note that these methods were originally proposed for other scenarios. In our simulations, we adapted them to point-to-point MIMO systems.

The effective achievable rates of the different methods are shown in Fig. 10(a), where we consider $M = 30$ reflecting elements, while the other simulation parameters are the same as those above. For the grouping-based method, we consider arranging the RIS elements into five groups, each of which has six elements. It can be seen from Fig. 10(a) that for a rapidly time-varying channel (e.g., $T \le 200$), the effective achievable rate is quite different. First of all, the AO algorithm shows

the worst performance, since it relies on an excessive pilot overhead for CSI acquisition. Furthermore, the performance of the AO algorithm can be improved by lumping together the adjacent elements into groups under rapidly time-varying channels. Interestingly, the random configuration maintains nearly the best performance in the face of rapidly time-varying channels, which is because the random configuration relies on the lowest pilot overhead, thus significantly improving the effective achievable rate. Compared to the performance penalty suffered by the AO algorithm, the reduced pilot overhead of the random configuration is more beneficial for rapidly time-varying channels. Additionally, the RIS configuration relying on statistical CSI attains further performance improvements over the random configuration under the minimum pilot overhead, but the performance gain attained depends on the quality of the channel statistics. As the channel's coherence time increases in case of slowly time-varying channels, the AO algorithm would gradually outperform the random configuration and becomes the best upon further increasing the channel's coherence time. We emphasize that the proposed algorithm is capable of flexibly adjusting the training overhead according to the specific coherence time, thus maximizing the effective achievable rate. For example, under the setups considered, we could set $Q = 1$ for $T \le 200$, and $Q = 5$ for $T > 200$, thus having the most energy-efficient communications all the time. The quantitative analysis of the optimal pilot overhead is beyond the scope of this paper and will be left for our future
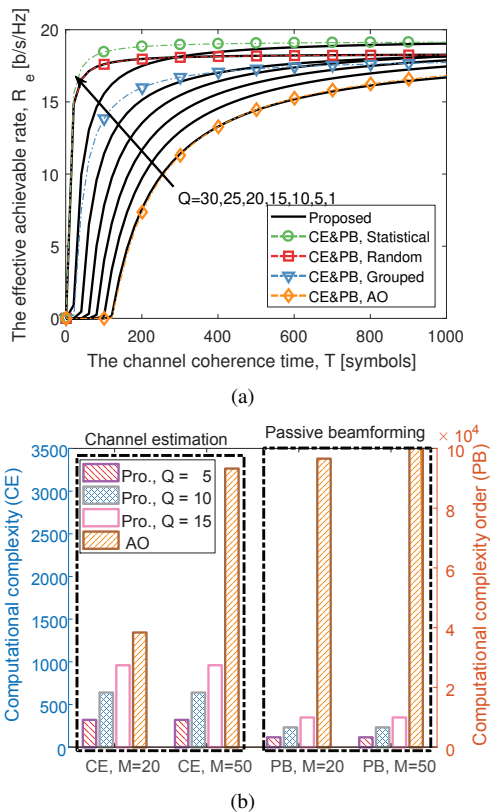
Fig. 10. (a) The effective achievable rate versus the channel coherence time. (b) The complexity comparison between the proposed scheme and the AO algorithm ($B = 2$, $N_i = 3$).

research topic.

Finally, we compare the computational complexity of the proposed scheme to that of the AO algorithm, as shown in Fig. 10(b), where we set $B = 2$ and $N_i = 3$. Please bear in mind that the complexity of channel estimation is evaluated in terms of the number of real-valued multiplications, while that of passive beamforming is assessed in terms of the complexity order associated with solving the optimization problems involved. It can be observed from Fig. 10(b) that the complexity of the proposed algorithm does not increase with the number of RIS elements, but that of the AO algorithm does. Specifically, the complexity order of the AO algorithm employed for passive beamforming increases quadratically with the number of RIS elements, which rapidly escalates and hence cannot be applied for massive RIS deployment. Furthermore, although the proposed algorithm increases with the number of training periods Q, it is still far lower than the complexity of the AO algorithm, especially for a large RIS having a lot of elements.

VIII. CONCLUSIONS

A low-complexity channel estimation and passive beamforming framework was proposed for RIS-based MIMO systems with discrete phase shifts at each reflecting element. In contrast to the existing schemes, the proposed arrangement partitions the channel training into several phases, where the RIS reflection coefficients are pre-designed and the effective superposed channel is estimated instead of separately estimating the direct channel and reflected channels. Based on this, on one hand, the active beamforming weights used at the transmitter are designed at low complexity. On the other hand, the optimization of the RIS reflection coefficients is performed by selecting the one that maximizes the achievable rate from the pre-designed training set. Furthermore, we proposed two configuration approaches for generating the training set, where the performance of the random configuration was used as a benchmarker of the proposed scheme. The scheme advocated is capable of striking a flexible trade-off between the achievable performance and the training overhead. In order to further improve the performance of the proposed solution, we conceived an improved configuration method by maximizing the Euclidean distance sum of all pairs of the reflection coefficient vector. Additionally, we elaborated on the advantages of the proposed framework in terms of reducing the complexity, pilot overhead, and signaling overhead. Finally, our simulations verify the advantages of the proposed algorithm over its existing counterparts, especially in the case of practical situations having imperfect CSI.

Nonetheless, some open issues await further investigations, one of which is the generation of the training set of the RIS reflection coefficients. Although we have proposed a pair of efficient configuration methods for generating the training set, it is possible to find a better training set for further improving the performance of the proposed algorithm. Additionally, in this paper, we adopted a decision center to select the training set, but future research may be able to exploit the limited training periods more effectively. Finally, the extension of the proposed method to multi-user scenarios and wideband systems forms part of our future research.

REFERENCES

[1] E. Basar, M. Di Renzo, J. De Rosny, M. Debbah, M. Alouini and R. Zhang, "Wireless communications through reconfigurable intelligent surfaces," *IEEE Access*, vol. 7, pp. 116753-116773, 2019.

[2] W. Tang, M. Chen, X. Chen, J. Dai, Y. Han, M. Di Renzo, Y. Zeng, S. Jin, Q. Cheng and T. J. Cui, "Wireless communications with reconfigurable intelligent surface: Path loss modeling and experimental measurement," *IEEE Trans. Wireless Commun.*, vol. 20, no. 1, pp. 421–439, Jan. 2021.

[3] C. Huang, S. Hu, G. C. Alexandropoulos, A. Zappone, C. Yuen, R. Zhang, M. D. Renzo and M. Debbah, "Holographic MIMO surfaces for 6G wireless networks: Opportunities, challenges, and trends," *IEEE Wireless Commun.*, vol. 27, no. 5, pp. 118-125, Oct. 2020.

[4] M. Di Renzo, A. Zappone, M. Debbah, M.-S. Alouini, C. Yuen, J. de Rosny and S. Tretyakov, "Smart radio environments empowered by reconfigurable intelligent surfaces: How it works, state of research, and the road ahead," *IEEE J. Sel. Areas Commun.*, vol. 38, no. 11, pp. 2450-2525, Nov. 2020.

[5] Q. Wu and R. Zhang, "Towards smart and reconfigurable environment: Intelligent reflecting surface aided wireless network," *IEEE Commun. Mag.*, vol. 58, no. 1, pp. 106-112, Jan. 2020.

[6] Y. Liang, R. Long, Q. Zhang, J. Chen, H. V. Cheng and H. Guo, "Large intelligent surface/antennas (LISA): Making reflective radios smart," *J. Commun. Inf. Net.*, vol. 4, no. 2, pp. 40-50, June 2019.

[7] S. Hu, F. Rusek and O. Edfors, "Beyond massive MIMO: The potential of data transmission with large intelligent surfaces," *IEEE Trans. Signal Process.*, vol. 66, no. 10, pp. 2746-2758, May 2018.

[8] J. Zhang, E. Bjornson, M. Matthaiou, D. W. K. Ng, H. Yang and D. J. Love, "Prospective multiple antenna technologies for beyond 5G," *IEEE J. Sel. Areas Commun.*, vol. 38, no. 8, pp. 1637-1660, Aug. 2020.

[9] M. Di Renzo, M. Debbah, D.-T. Phan-Huy, A. Zappone, M.-S. Alouini, C. Yuen, V. Sciancalepore, G. C. Alexandropoulos, J. Hoydis, H. Gacanin, J. de Rosny, A. Bounceur, G. Lerosey and M. Fink. "Smart radio environments empowered by reconfigurable AI meta-surfaces: An idea whose time has come," *J. Wireless Commun. Netw.*, 2019.

[10] Q. Wu, S. Zhang, B. Zheng, C. You and R. Zhang, "Intelligent reflecting surface aided wireless communications: A tutorial," *IEEE Trans. Commun.*, vol. 69, no. 5, pp. 3313-3351, May 2021.

[11] C. Huang, A. Zappone, G. C. Alexandropoulos, M. Debbah and C. Yuen, "Reconfigurable intelligent surfaces for energy efficiency in wireless communication," *IEEE Trans. Wireless Commun.*, vol. 18, no. 8, pp. 4157-4170, Aug. 2019.

[12] Q. Wu and R. Zhang, "Intelligent reflecting surface enhanced wireless network via joint active and passive beamforming," *IEEE Trans. Wireless Commun.*, vol. 18, no. 11, pp. 5394-5409, Nov. 2019.

[13] E. Bjornson, O. Ozdogan and E. G. Larsson, "Intelligent reflecting surface versus decode-and-forward: How large surfaces are needed to beat relaying?," *IEEE Wireless Commun. Lett.*, vol. 9, no. 2, pp. 244-248, Feb. 2020.

[14] W. Saad, M. Bennis and M. Chen, "A vision of 6G wireless systems: Applications, trends, technologies, and open research problems," *IEEE Netw.*, vol. 34, no. 3, pp. 134-142, Jun. 2020.

[15] B. Zheng and R. Zhang, "Intelligent reflecting surface-enhanced OFDM: Channel estimation and reflection optimization," *IEEE Wireless Commun. Lett.*, vol. 9, no. 4, pp. 518-522, Apr. 2020.

[16] D. Mishra and H. Johansson, "Channel estimation and low-complexity beamforming design for passive intelligent surface assisted MISO wireless energy transfer," *2019 IEEE Int. Conf. Acoust., Speech and Signal Process. (ICASSP)*, Brighton, United Kingdom, 2019, pp. 4659-4663.

[17] T. L. Jensen and E. De Carvalho, "An optimal channel estimation scheme for intelligent reflecting surfaces based on a minimum variance unbiased estimator," *2020 IEEE Int. Conf. Acoust., Speech and Signal Process. (ICASSP)*, Barcelona, Spain, 2020, pp. 5000-5004.

[18] J. An, L. Wang, C. Xu, L. Gan and L. Hanzo, "Optimal pilot power based channel estimation improves the throughput of intelligent reflective surface assisted systems," *IEEE Trans. Veh. Technol.*, vol. 69, no. 12, pp. 16202-16206, Dec. 2020.

[19] Z. Wang, L. Liu and S. Cui, "Channel estimation for intelligent reflecting surface assisted multiuser communications: Framework, algorithms, and analysis," *IEEE Trans. Wireless Commun.*, vol. 19, no. 10, pp. 6607-6620, Oct. 2020.

[20] J. Chen, Y.-C. Liang, H. Victor Cheng, W. Yu, "Channel estimation for reconfigurable intelligent surface aided multi-user MIMO systems," arXiv: 1912.03619, 2019.

[21] C. You, B. Zheng and R. Zhang, "Channel estimation and passive beamforming for intelligent reflecting surface: Discrete phase shift and progressive refinement," *IEEE J. Sel. Areas Commun.*, vol. 38, no. 11, pp. 2604-2620, Nov. 2020.

[22] S. Gong, X. Lu, D. T. Hoang, D. Niyato, L. Shu, D. I. Kim and Y. -C. Liang, "Toward smart wireless communications via intelligent reflecting surfaces: A contemporary survey," *IEEE Commun. Surveys Tuts.*, vol. 22, no. 4, pp. 2283-2314, Fourth quarter 2020.

[23] Q. Wu and R. Zhang, "Beamforming optimization for wireless network aided by intelligent reflecting surface with discrete phase shifts," *IEEE Trans. Commun.*, vol. 68, no. 3, pp. 1838-1851, Mar. 2020.

[24] S. Zhang and R. Zhang, "Capacity characterization for intelligent reflecting surface aided MIMO communication," *IEEE J. Sel. Areas Commun.*, vol. 38, no. 8, pp. 1823-1838, Aug. 2020.

[25] H. Guo, Y.-C. Liang, J. Chen and E. G. Larsson, "Weighted sum-rate optimization for intelligent reflecting surface enhanced wireless networks," arXiv: 1905.07920, 2019.

[26] S. Abeywickrama, R. Zhang, Q. Wu and C. Yuen, "Intelligent reflecting surface: Practical phase shift model and beamforming optimization," *IEEE Trans. Commun.*, vol. 68, no. 9, pp. 5849-5863, Sep. 2020.

[27] Y. Han, W. Tang, S. Jin, C. Wen and X. Ma, "Large intelligent surface-assisted wireless communication exploiting statistical CSI," *IEEE Trans. Veh. Technol.*, vol. 68, no. 8, pp. 8238-8242, Aug. 2019.

[28] T. Van Chien, A. K. Papazafeiropoulos, L. T. Tu, R. Chopra, S. Chatzinotas and B. Ottersten, "Outage probability analysis of IRS-assisted systems under spatially correlated channels," *IEEE Wireless Commun. Lett.*, Early Access, 2021.

[29] T. Van Chien, H. Q. Ngo, S. Chatzinotas, M. Di Renzo, and B. Ottersten, "Reconfigurable intelligent surface-assisted cell-free massive MIMO systems over spatially-correlated channels," arXiv: 2104.08648, 2021.

[30] M. Hua, Q. Wu, D. W. K. Ng, J. Zhao and L. Yang, "Intelligent reflecting surface-aided joint processing coordinated multipoint transmission," *IEEE Trans. Commun.*, vol. 69, no. 3, pp. 1650-1665, Mar. 2021.

[31] Z. Zhou, N. Ge, Z. Wang and L. Hanzo, "Joint transmit precoding and reconfigurable intelligent surface phase adjustment: A decomposition-aided channel estimation approach," *IEEE Trans. Commun.*, vol. 69, no. 2, pp. 1228-1243, Feb. 2021.

[32] A. Zappone, M. Di Renzo, F. Shams, X. Qian and M. Debbah, "Overhead-aware design of reconfigurable intelligent surfaces in smart radio environments," *IEEE Trans. Wireless Commun.*, vol. 20, no. 1, pp. 126-141, Jan. 2021.

[33] Y. Yang, B. Zheng, S. Zhang and R. Zhang, "Intelligent reflecting surface meets OFDM: Protocol design and rate maximization," *IEEE Trans. Commun.*, vol. 68, no. 7, pp. 4522-4535, Jul. 2020.

[34] J. Chen, Y. Liang, Y. Pei and H. Guo, "Intelligent reflecting surface: A programmable wireless environment for physical layer security," *IEEE Access*, vol. 7, pp. 82599-82612, 2019.

[35] H. Shen, W. Xu, S. Gong, Z. He and C. Zhao, "Secrecy rate maximization for intelligent reflecting surface assisted multi-antenna communications," *IEEE Commun. Lett.*, vol. 23, no. 9, pp. 1488-1492, Sep. 2019.

[36] P. Wang, J. Fang, X. Yuan, Z. Chen and H. Li, "Intelligent reflecting surface-assisted millimeter wave communications: Joint active and passive precoding design," *IEEE Trans. Veh. Technol.*, vol. 69, no. 12, pp. 14960-14973, Dec. 2020.

[37] S. Li, B. Duo, X. Yuan, Y. Liang and M. Di Renzo, "Reconfigurable intelligent surface assisted UAV communication: Joint trajectory design and passive beamforming," *IEEE Wireless Commun. Lett.*, vol. 9, no. 5, pp. 716-720, May 2020.

[38] C. Xu, T. Bai, J. Zhang, R. Rajashekar, R. G. Maunder, Z. Wang and L. Hanzo, "Adaptive coherent/non-coherent spatial modulation aided unmanned aircraft systems," *IEEE Wireless Commun.*, vol. 26, no. 4, pp. 170-177, Aug. 2019.

[39] E. Basar, "Reconfigurable intelligent surface-based index modulation: A new beyond MIMO paradigm for 6G," *IEEE Trans. Commun.*, vol. 68, no. 5, pp. 3187-3196, May 2020.

[40] C. Huang, R. Mo and C. Yuen, "Reconfigurable intelligent surface assisted multiuser MISO systems exploiting deep reinforcement learning," *IEEE J. Sel. Areas Commun.*, vol. 38, no. 8, pp. 1839-1850, Aug. 2020.

[41] G. Yang, X. Xu and Y. Liang, "Intelligent reflecting surface assisted non-orthogonal multiple access," *2020 IEEE Wireless Commun. and Netw. Conf. (WCNC)*, pp. 1-6, 2020.

[42] Q. Wu and R. Zhang, "Weighted sum power maximization for intelligent reflecting surface aided SWIPT," *IEEE Wireless Commun. Lett.*, vol. 9, no. 5, pp. 586-590, May 2020.

[43] C. Pan, H. Ren, K. Wang, M. Elkashlan, A. Nallanathan, J. Wang and L. Hanzo, "Intelligent reflecting surface aided MIMO broadcasting for simultaneous wireless information and power transfer," *IEEE J. Sel. Areas Commun.*, vol. 38, no. 8, pp. 1719-1734, Aug. 2020.

[44] C. Pan, H. Ren, K. Wang, W. Xu, M. Elkashlan, A. Nallanathan and L. Hanzo, "Multicell MIMO communications relying on intelligent reflecting surfaces," *IEEE Trans. Wireless Commun.*, vol. 19, no. 8, pp. 5218–5233, Aug. 2020.

[45] Z. Zhang and L. Dai, "A joint precoding framework for wideband reconfigurable intelligent surface-aided cell-free network," arXiv: 2002.03744, 2020.

[46] M. Biguesh and A. B. Gershman, "Training-based MIMO channel estimation: A study of estimator tradeoffs and optimal training signals," *IEEE Trans. Signal Process.*, vol. 54, no. 3, pp. 884-893, Mar. 2006.

[47] D. Tse and P. Viswanath, "Fundamentals of wireless communication," *Cambridge university press*, 2005.

[48] A. Renyi, "On the theory of order statistics," *Acta Mathematica Academiae Scientiarum Hungarica*, vol. 4, pp. 191-231, 1953.

[49] J. Havil, "Gamma: exploring Euler's constant," *The Australian Mathematical Society*, 2003.

[50] J. An, C. Xu, L. Wang, Y. Liu, L. Gan, and L. Hanzo, "Joint training of the superimposed direct and reflected links in reconfigurable intelligent surface assisted multiuser communications," arXiv: 2105.14484, 2021.